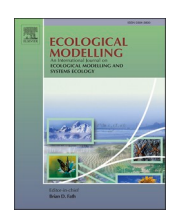
\$ SUPER

Contents lists available at ScienceDirect

Ecological Modelling

journal homepage: www.elsevier.com/locate/ecolmodel





Simulating the fate of compost-derived nutrients in an urban garden

Gaston E. Small a,b,*, Marisa Smedsrud b,c, Ivan Jimenez a, Eric Chapman a

- ^a Biology Department, University of St. Thomas, Saint Paul, MN 55105, USA
- ^b Department of Earth, Environment, and Society, University of St. Thomas, Saint Paul, MN 55105, USA
- ^c University of Michigan School for Environment and Sustainability, Ann Arbor, Michigan, USA

ARTICLE INFO

Keywords:
Compost
Model
Agroecosystem
Nitrogen
Carbon
Phosphorus

ABSTRACT

The application of compost to urban vegetable gardens presents an opportunity to recycle nutrients from the urban waste stream back into the human food system. However, many gardeners apply phosphorus (P) in the form of compost at a rate that far exceeds what crops can take up. The fate of this P—whether stored in soil, taken up by plants, or exported through leachate, depends on the dynamics of water, carbon (C), and nitrogen (N) in this agroecosystem. We developed a model representing these four currencies (C, N, P, water) in urban garden soils, that was parameterized and validated using data from four years of data from an experiment in which high or low amounts of labile manure-based compost, or recalcitrant municipal compost, are added to garden plots annually. We used the model to simulate the effects of longer-term (10-year) additions of labile or recalcitrant compost at low, medium, or high levels (based on previously reported survey data for Minneapolis-Saint Paul, Minnesota), tracking the fate of added N and P, as well as calculating net C sequestration. The fraction of compost nutrients recovered over 10 years ranged from 3 to 47% (N) and 4–67% (P) with higher efficiencies associated with lower input rates and for recalcitrant compost. Approximately half of added C was ultimately respired by soil microbes, while C sequestration from crop growth was much lower than soil respiration. This model provides a tool for understanding how management decisions and climate control nutrient recycling and loss via leachate from compost application in urban agroecosystems.

1. Introduction

1.1. Nutrient recycling and loss from compost in urban agriculture

Cities are characterized as open systems, requiring importation of food and other resources, and producing wastes that end up in discharged wastewater, landfills, or in air, water, or soil pollution (Rees and Wackernagel 1994). Urban sustainability ultimately requires the creation of circular economies in which waste products are converted into new resources (Childers et al., 2011; Burger et al., 2012). Many metropolitan areas are expanding composting to keep organics waste out of landfills while producing a useful end-product that is used in gardening and landscaping as a soil amendment. Food production in many cities has also increased in recent decades, and urban farms and vegetable gardens present an opportunity to recycle nutrients from food waste back into the human food system through compost application (Metson and Bennett 2015).

While compost application in urban gardens creates the potential for nutrient recycling, it also creates the potential for nutrient loss to the environment, if only a fraction of nutrients applied to soil are recovered by crops. Many composts have high nitrogen (N) to phosphorus (P) ratios relative to crop requirements, such that applying compost to fulfill crop N requirements can result in overapplication of P by 5-fold or more (Kleinman et al., 2007, 2011). Moreover, many urban gardeners and farmers apply compost at much higher levels because of perceived environmental benefits and lack of economic and regulatory disincentives. The few available published nutrient budgets from urban agriculture systems indicate that compost applications result in N and especially P input rates that far exceed crop requirements (e.g., Smith 2001, Cofie et al., 2003, Graefe et al., 2008, Metson and Bennet 2015, Wielemaker et al., 2019). Our previous work in Minneapolis-Saint Paul, Minnesota, documented high compost application rates and low nutrient use efficiencies in urban gardens (median values of 2.5% for P, 5.0% for N) (Small et al., 2019a), with garden soils having levels of plant-available P far higher than recommended levels that increased with garden age (Small et al., 2019a), indicating buildup over time. Even though urban farms and gardens make up a small fraction (typically <1%) of urban land area, compost inputs into this small area may

^{*} Corresponding author at: Biology Department, University of St. Thomas, Saint Paul, MN 55105, USA. *E-mail address:* gaston.small@stthomas.edu (G.E. Small).

constitute one of the largest inputs of P onto the urban landscape (Small et al., 2019a). If retention of excess P in the soil is low, compost inputs to urban gardens can lead to high rates of P export urban watersheds as leachate and stormwater runoff (Small et al., 2023), potentially contributing to eutrophication of downstream water bodies.

Published values indicate a wide range of nutrient loss rates that are not always correlated with inputs at annual timescales (van de Vlasakker et al. 2022), suggesting complex controls on longer-term nutrient dynamics that are influenced by interactions among physical (e.g., soil characteristics, water inputs) and biological factors (e.g., microbial mineralization of compost, crop uptake of nutrients). A multi-currency ecosystem model is needed to better understand these interactions and to allow for simulations of sufficient temporal duration to evaluate long-term fate of compost-bound P. Understanding these controls on recycling, retention, and export of compost-derived nutrients is essential in order for compost-based urban agriculture to maximize ecosystem services while minimizing environmental consequences.

1.2. Factors controlling the fate of compost-derived nutrients

The source of compost is likely to be an important determinant of the fate of compost-derived nutrients. Compost made from yard waste and other municipal organic sources is commonly used in urban agriculture, as is compost made from animal manure (Wielemaker et al., 2019). Manure-based composts have been associated with high leaching rates of N and P (Graefe et al., 2008), likely due to high input rates combined with the lability of this material (Chu et al., 2007; Chang et al., 2010; Sandhu et al., 2019). Highly labile manure compost can result in rapid mineralization and loss of nutrients, whereas slower decomposing compost can lead to higher nutrient immobilization in soil microbial biomass (Aoyama and Nozawa 2012).

Compost-bound nutrients are mineralized by microbial activity rates which depend on compost carbon quality (Luu et al., 2022) and environmental conditions including soil moisture and temperature (Cambardella et al., 2003; Yuste et al., 2007). Soil moisture, in turn, is influenced by water inputs from precipitation or irrigation, and loss from evapotranspiration or leachate. Soil water-holding capacity controls rates of evapotranspiration and leachate and is weakly related to soil organic matter content (Minasny and McBratney, 2017).

Plant-available N and P are taken up by crop roots based on crop growth rate and nutrient demand, and environmental conditions such as soil moisture (Chtouki et al., 2022). Nitrogen loss from agricultural soils occurs via leachate (Di and Cameron 2002) and from volatilization of ammonia (Xing and Zhu 2000). While P binds more tightly to soil minerals compared to N, loss of dissolved P does occur through leachate (Turner and Haygarth 2000).

Notably, in this agroecological system, the fates of water (soil moisture), organic carbon, nitrogen, and phosphorus are interconnected. Soil moisture depends on soil organic carbon and rates of transpiration by crops. Soil organic carbon depends on microbial mineralization rates influenced by soil moisture and nutrient availability. Soil N and P concentrations depend on rates of microbial mineralization of compost, uptake by crops, and export via leachate. Crop growth depends on availability of soil moisture, and N availability, among other factors. In order to understand recycling and retention of P applied as compost to urban gardens, it is therefore necessary to also understand the dynamics of water, carbon, and nitrogen.

1.3. Results from empirical measurements of compost-derived nutrients in an urban garden

In replicated raised bed garden plots, we found that high compost inputs can result in high losses of P via leachate flux (Small et al., 2018), and that native soils below garden plots showed P accumulation (Small et al., 2019b) resulting from mobilized P. However, we also found that compost applications targeted towards crop nutrient demand can

maintain crop yields while minimizing nutrient loss from leachate (Shrestha et al., 2020). Plots receiving labile manure compost had higher leachate P losses compared to plots receiving inputs of more recalcitrant municipal compost, and a lower buildup of plant-available P in soils as a result of these losses (Shrestha et al., 2020). Results from these experiments also show that urban gardens have high evapotranspiration rates relative to lawns (Small et al., 2020) and that compost application rates can be an important control on the storage and fate of water in gardens (Chapman et al., 2022).

The annual nutrient use efficiency (mass of nutrients recovered in crops / mass of nutrients added as compost) calculations from empirical measurements (Small et al., 2018; Shrestha et al., 2020) and gardener surveys (Small et al., 2019a) that we have previously reported provide a coarse but useful indicator of nutrient recycling; this metric is an overly simplistic representation of a dynamic system with long time lags resulting from a potentially large, slow-turnover pool of soil nutrients. Nutrients added as compost may be mineralized over a period of years, where they may be stored in soil, taken up by crops, or exported through leachate. As a result, soil nutrient availability and crop uptake in any given year reflects the history of inputs and environmental conditions experienced over a multi-year period. Dynamic models are needed to better understand the coupled dynamics of organic matter decomposition, crop growth, and the retention of water and nutrients in soil, that characterize this agroecosystem.

1.4. Objective of the current study

The goals of this study are to create a dynamic ecosystem model of water, organic C, N and P for a small-scale urban vegetable garden; to parameterize and validate this model using empirical data; and to use the model to track the fate of compost-derived P over ten years at a range of different compost input rates.

We previously developed a mass-balance hydrology model that synthesized four years of empirical data from the experiments described above to simulate the effect of compost amendments on water storage, leachate, and evapotranspiration (Chapman et al., 2022). Simulations illustrated that compost-amended garden soil has a greater capacity to retain moisture and ultimately export relatively more water through evapotranspiration instead of leachate. Here, we have built upon this model to add sub-models representing the dynamics of N, P, and organic

2. Materials and methods

2.1. Experimental design and empirical data collection

A multi-year experiment to measure the fate of compost-derived N and P in urban vegetable gardens began in 2017 in the campus research garden at the University of St. Thomas in Saint Paul, Minnesota. The garden includes 32 replicate raised beds measuring 4 m² and 0.3 m deep. At the start of this current study, soil was homogenized across all plots. Each bed is divided into four subplots (1 m²) in which the following crops were planted and rotated annually: 1) carrots; 2) bush beans; 3) bell peppers; and 4) cabbage (2017) or collards (2018-2022). Each plot was randomly assigned to one of six soil amendment treatments (the four subplots within each plot received the same treatment), as described by Shrestha et al. (2020). Soil treatments consist of: 1) a control treatment in which no compost or fertilizer is added (no fertilizer); 2) synthetic fertilizer targeted to meet crop N and P demand (synthetic); 3) a higher input rate of labile manure compost targeted to meet crop N demand (high-input manure); 4) a lower input rate of labile manure compost targeted to meet crop P demand, supplemented with additional synthetic N fertilizer (low-input manure); 5) a higher input rate of recalcitrant municipal compost targeted to meet crop N demand (high-input municipal); and 6) a lower input rate of recalcitrant municipal compost targeted to meet crop P demand, supplemented with

additional synthetic N fertilizer (low-input municipal). Input rates of compost and supplemental fertilizer are described in Appendix 1.

Response variables include harvested biomass, soil organic matter and plant-available nutrient concentrations (NH₄—N, NO₃—N, Bray P), leachate volume and dissolved nutrient concentrations (NH₄—N, NO₃—N, PO₄-P), soil moisture, and soil respiration. Meteorological data are also recorded onsite. We previously published nutrient budgets from the first two years (2017–2018) of the experiment (Shrestha et al., 2020) and soil moisture and leachate volume from the first three years of the study (Chapman et al., 2022). Data from the first six years of the experiment are publicly available (Small & Shrestha 2023).

2.2. Model currency and system boundaries

We created a dynamic mass-balance model representing stocks and flows of water, organic C, N, and P in the experimental garden plots (Fig. 1). The system boundary was represented as one experimental raised-bed garden subplot, with an area of $1 \mathrm{m}^2$ and soil depth of 0.3 m (total soil volume 300 L). The simulation was run from 27 May 2017 – 25 May 2027 (3650 days), encompassing 10 growing seasons, with a time step of 1 day. The model was run using Stella Architect (1.5.2) using the Euler integration method.

2.3. Hydrology submodel

The hydrology submodel, previously described in Chapman et al. (2022), represents soil moisture (SM) as volume of water (L) within a 1 m x 1 m x 0.3 m (300 L) experimental garden plot:

dSM/dt = precipitation + supplemental irrigation - water leachate - evapotranspiration

Daily precipitation and supplemental irrigation (mm/d, or $L/m^2/d$) were inputs to the model based on recorded data. Water leachate (mm/d, or $L/m^2/d$) was modeled based on the difference between modeled soil moisture and soil water capacity. Soil water capacity was modeled as a function of soil% organic matter, based on the observed relationship between the mean% organic matter for each soil amendment treatment and the maximum observed soil moisture in that treatment (R^2 =0.57). Water storage in excess of water capacity was assumed to be exported as leachate.

We calculated evapotranspiration (mm/d, or L/m²/d) based on the Penman-Monteith equation (Zotarelli et al., 2010), using mean daily solar radiation, maximum and minimum relative humidity, maximum and minimum temperature, and mean wind speed as inputs. The calculated reference evapotranspiration rate (representing turfgrass) was converted to potential crop evapotranspiration using seasonally

varying crop coefficients ranging from 0.55 to 1.2, with maximum values in the middle of the growing season (based on values reported in Saher et al. 2021). Potential crop evapotranspiration was multiplied by a correction factor, $k_{\rm s}$, that is a function of soil moisture (Zotarelli et al., 2010), adjusting ET downward in drier soil. Between soil moisture values of 6% and 21%, $k_{\rm s}$ increases linearly from 0 to 1. During the parameterization process, we adjusted calculated ET using a correction factor of 2 to achieve a good correspondence between modeled and observed soil moisture and cumulative leachate values.

2.4. Plant growth submodel

Crop mass-specific growth rate (kGrowth) was represented as a function of five variables. A crop-specific maximum growth rate (kmaxGrowth), soil moisture (measured % moisture), daily minimum temperature (Tmin); daily mean solar intensity (Rs); and soil plantavailable N. For kmaxGrowth, a time series input was used to represent the annual crop rotations and values were calibrated manually to match observed harvest values; we used values of 0.07 d^{-1} for peppers, $0.05 d^{-1}$ for beans, $0.15 d^{-1}$ for collard greens, and $0.07 d^{-1}$ for carrots. Graphical functions were used to convert measured % moisture, Tmin, Rs, and soil plant-available N into index values ranging between 0 and 1, which were in turn multiplied by the maximum growth rate. The relative growth rate due to temperature (kTempGrowth) was assumed to equal 1 at daily minimum temperatures above 15.5 °C, and 0 at daily minimum temperatures below 2.0 °C. The relative growth rate due to soil moisture was represented as ks (also used in the calculation for ET), with values of 1 for any measured soil moisture >2.5%, and 0 for measured soil moisture <2.5%. The relative growth rate due to light (kLight) was represented by a graphical function as 1 for values $> 8.5 \text{ MJ/m}^2/\text{d}$ and 0 for values <1.5 MJ/m²/d. The relative growth rate due to plantavailable N (kNgrowth) was represented by a graphical function as 1 for values >20 PPM, and 0 for values <1 PPM. The mass specific growth rate of crops was represented as:

kGrowth = kmaxGrowth * kTempGrowth * ks * kLight * kNgrowth

2.5. Decomposition rate submodel

The mass-specific decomposition rate of organic matter, kDecomp, was a variable represented as a maximum decomposition rate (kMaxdecomp), modified by functions based on daily minimum temperature (Tmin) and soil moisture. The relative decomposition rate due to temperature (kTempDecomp) was assumed to equal 1 at daily minimum temperatures above 25 $^{\circ}$ C, and 0 at daily minimum temperatures below

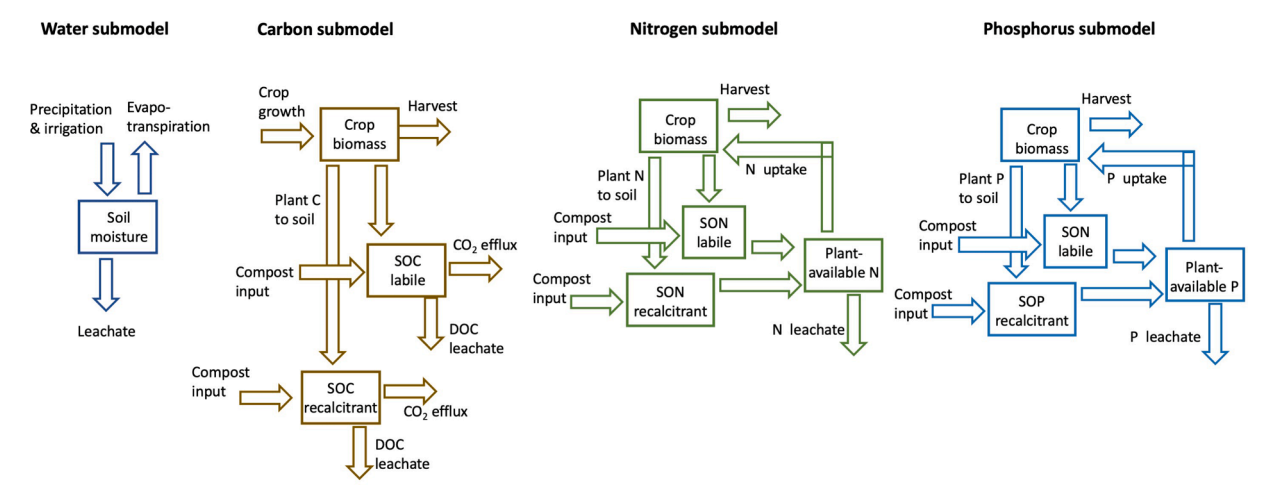


Fig. 1. Conceptual model of garden ecosystem, representing stocks and flows of water, organic carbon, nitrogen, and phosphorus.

 $5\,^{\circ}$ C. The relative decomposition rate due to soil moisture (kMoistureDecomp) was assumed to be equal to 1 at soil moisture values >22%, declining to 0 at 0% moisture. The mass specific decomposition rate of organic matter was represented as:

kDecomp = kMaxdecomp * kTempDecomp * kMoistureDecomp

2.6. Organic carbon submodel

Organic carbon was represented by three stocks: Crop Biomass Carbon (CBC), Labile Soil Organic Carbon (LSOC), and Recalcitrant Soil Organic Carbon (RSOC).

CBC was modeled as:

```
\label{eq:dcbcdt} \begin{split} dCBC/dt &= (planting\_input\_C) + (crop\_growth\_C) - (harvest\_C) - (crop\_C\_to\_soil) \end{split}
```

Planting input C was represented as a small annual input (1 g C/m^2) on June 1 of each simulation year, representing the planting of seedlings. Crop growth C was represented as:

```
\label{eq:crop_bounds} Crop\ growth\ C = Crop\ biomass\ C\ * kGrowth\ * (kmaxBiomass\ - Crop\_Biomass\ - Crop
```

where kmaxBiomass represented the maximum biomass value of a given crop (e.g., due to shading). kmaxBiomass values were calibrated manually and set as $115~{\rm g~C/m}^2$ for peppers, $140~{\rm g~C/m}^2$ for beans, $360~{\rm g~C/m}^2$ for collards, and $500~{\rm g~C/m}^2$ for carrots.

The Harvest C flow simulated the removal of 95% of crop biomass on October 15 of each simulated year. The crop C to soil flow was simulated as a constant fraction (kexC), 0.5% of crop growth C, representing root exudate flows, and the remaining 5% of crop biomass after harvest.

Labile soil organic carbon (LSOC) was modeled as:

```
 \label{eq:dlsoc} \begin{split} dLSOC/dt &= (labile\_C\_input) + (crop\_C\_to\_soil\_Labile) - (DOC\_leachate\_Labile) - (labile\_CO_2\_efflux) \end{split}
```

Recalcitrant soil organic carbon (RSOC) was modeled as:

```
\begin{split} dRSOC/dt &= (recalcitrant\_C\_input) + (crop\_C\_to\_soil\_Recalcitrant) - (DOC\_leachate\_Recalcitrant) - (recalcitrant\_CO_2\_efflux) \end{split}
```

The LSOC and RSOC stocks received inputs of labile C from compost, represented as a time-series input function with compost inputs occurring on 28 May of each simulated year. The compost%labile variable determined the amount of compost C inputs added to SOC Labile and SOC recalcitrant stocks; manure compost was set at 50% labile, and municipal compost was set at 25% labile. Similarly, the crop C to soil flow was partitioned with 10% assumed to go into labile SOC and 90% to recalcitrant SOC. Dissolved organic carbon (DOC) leachate was exported from SOC stocks, represented as the water leachate flux multiplied by the labile and recalcitrant DOC concentrations. Labile DOC concentration was represented as a function of the SOC Labile stock, with a maximum value of 200 mg C/L at labile SOC stocks > 5000 g/m². Recalcitrant DOC concentration was represented as a function of the SOC Recalcitrant stock, with a maximum value of 10 mg C/L at recalcitrant SOC values > 8000 g/m². Labile CO₂ efflux was represented as the product of kDecomp (from the decomposition rate submodel) and the LSOC stock. Recalcitrant CO2 efflux was represented as the product of kDecomp, the RSOC stock, and kRecalDecompFactor, which was set as 0.018.

2.7. Nitrogen submodel

The N submodel had four stocks: labile soil organic N (LSON), recalcitrant soil organic N (RSON), plant-available N, and plant N. The two SON stocks were modeled as:

```
dLSON/dt = (compost_N_input_Labile) + (crop_N_to_soil_Labile) - (N_mineralization_Labile)
```

and

```
\begin{split} dRSON/dt &= (compost\_N\_input\_Recalcitrant) + (crop\_N\_to\_soil\_Recalcitrant) - (N\_mineralization\_recalcitrant) \end{split}
```

The two crop N to soil fluxes were based on the crop_C_to_soil fluxes described above, divided by the crop C:N ratio. Crop C:N was represented as a time-series function based on simulated crop rotations, with peppers having a C:N (mass ratio) value of 14, beans 10, collards 14, and carrots 20. Compost N input was represented as a time-series function as described above, and partitioned into LSON and RSON stocks based on the compost_%labile parameter. The N_mineralization_labile flux was modeled as the product of kDecomp and the LSON stock. The N_mineralization_recalcitrant flux was represented as the product of KDecomp, the RSON stock, and kRecalDecompFactor, as described above.

The plant-available N stock was modeled as:

```
 dPlant-available\_N/dt = (inorg\_N\_input) + (N\_mineralization\_labile) + (N\_mineralization\_recalcitrant) - (gaseous\_N\_loss) - (N\_leachate) - (Plant\_N\_uptake)
```

Inorg_N_input was a time-series input representing the addition of synthetic N fertilizer, which occurred as 5 inputs separated by 2-week intervals in each growing season in the Synthetic Fertilizer, Manure P, and Municipal P experimental soil input treatments. Gaseous_N_loss was simulated as a constant fraction of the plant-available N stock, kNgasloss, fit by manual calibration and set at 0.017 d^{-1} . N_leachate was calculated as the product of the water leachate flux and the leachate N concentration. Leachate N concentration was represented as Plant-available N / soil moisture. Plant_N_uptake was represented as crop_growth_C / crop_C:N. The plant-N stock was modeled as:

```
dPlant\_N/dt = (planting\_N\_input) + (Plant\_N\_uptake) - (harvest\_N)
```

Planting_N_input was represented as planting_C_input / crop_C:N. Harvest_N was represented as harvest_C / crop_C:N.

2.8. Phosphorus submodel

The P submodel had four stocks, labile soil organic P (LSOP), recalcitrant soil organic P (RSOP), plant-available P, and Plant P.

The two SOP stocks were modeled as:

```
 dLSOP/dt = (compost\_P\_input\_Labile) + (Crop\_P\_to\_soil\_Labile) - (P\_mineralization\_Labile) \\
```

and

```
\label{eq:drsop} \begin{split} dRSOP/dt &= (compost\_P\_input\_Recalcitrant) + (Crop\_P\_to\_soil\_Recalcitrant) - (P\_mineralization\_Recalcitrant). \end{split}
```

Complete model equations are available in Appendix 2. An interactive version of this model is available at $\frac{\text{https://exchange.iseesystems.}}{\text{com/public/gaston-small/urban-garden-mass-balance-model/index.}}$ $\frac{\text{html.}}{\text{html.}}$

Time series input data are available in Appendix 3. Meteorological input data from 27 May 2017–26 May 2021 was taken from direct measurements at the research garden, with the exception of two gaps: 28–28 June 2018 (3 days), and 4 June-11 July 2019 (38 days). For those dates, meteorological parameter values were taken from the MSP airport (Minnesota DNR (2003)). For model days from 27 May 2021–26 May 2025, meteorological data was taken from the same date four years earlier. For model days after 26 May 2025, meteorological data was taken from the same date eight years before.

2.9. Tracer N and P simulation

We simulated the fate of compost-bound N and P added to the garden in year 1, over the 10-year simulation period, as if this material were an isotopically labeled tracer. We created a parallel stock-and-flow model for the tracer N and P. Flows in the tracer models were based on the turnover rate of the actual N and P models, so that the fraction of a stock moving through a given flow in the N or P submodel in a given timestep was equivalent to the fraction of N or P tracer moving from that same stock through that flow. The tracer submodel was initialized with 100 units of N and P that were divided among labile and recalcitrant soil organic compartments according to the "compost%labile" parameter. All other stocks were initially set to 0, so that the tracer submodel tracks the fate of this initial pool of organic N and P.

2.10. Model parameterization, verification and sensitivity analysis

The model was parameterized by manually adjusting parameters within reasonable ranges, fitting observed data for each of the six experimental soil input treatments to model output for the A subplots for four growing seasons (2017–2020). Model output was compared to empirical measurements for the following variables: soil moisture, cumulative leachate volume, soil $\rm CO_2$ flux, harvested biomass (in terms of C), soil% organic matter (loss-on-ignition method), plant-available N (NO₃-N + NH₄-N.), plant-available P (Bray P), cumulative leachate N (NO₃-N. + NH₄-N.) flux, and cumulative leachate P (PO₄-P) flux. Model parameters were adjusted iteratively until model output values followed temporal dynamics of observed values and magnitudes of all model output values were as close as possible (at least within an order of magnitude) of observed values. Comparisons of model output to empirical values are shown in Appendix 4.

We used three independent datasets from B subplots (which used a different crop rotation, with beans grown in 2017, collards in 2018, carrots in 2019, and peppers in 2020) for model verification. Compost input values and crop parameters for the model were updated accordingly, and we compared observed values with model output for harvested biomass C, cumulative N leachate, and cumulative P leachate to assess model performance. Model verification results are shown in Appendix 5. Model fit was assessed by comparing magnitude and temporal dynamics of model output and observed values, comparing relative difference across experimental treatments, and evaluating the correspondence between model output and observed values using Model II regression using the 'Imodel2' package in R.

A sensitivity analysis was conducted following the procedure outlined in Jørgensen and Bendoricchio (2001), in which 18 model parameters were adjusted to either 50% lower, 10% lower, 10% greater, or 50% greater than original values, and the model was run for the 10 year simulation period. The relative change in eight different cumulative model output variables (evapotranspiration, leachate volume, harvest C, CO_2 flux, N use efficiency, N leachate, P use efficiency, P leachate) was calculated. Results of the sensitivity analysis are shown in Appendix 6.

2.11. 10-year simulations

We used the model to simulate the long-term (10-year) dynamics of applying labile manure-based compost or recalcitrant municipal compost, at either low, medium, or high levels. These input rates are based on documented compost input rates for gardeners in the Minneapolis-St. Paul metropolitan area, reported by Small et al. (2019a), with low input rates corresponding to 25th percentile, medium input rates corresponding to median, and high input corresponding to 75th percentile. We also include a simulation of no soil amendments over 10 years. We report cumulative mass balance of N, P, and C for each of these seven scenarios. We also simulate concentrations of plant-available N and P over time, and we use the tracer submodel to track the fate of N and P from compost added at the start of the

experiment.

3. Results

3.1. Model calibration and verification

The model was generally successful in approximating observed values, representing differences among treatments, and seasonal and interannual trends for most variables (Appendix 4) while adhering to the constraints of mass balance for four different currencies. As previously reported (Chapman et al., 2022), modeled values for soil moisture (Appendix 4.1) and leachate volume (Appendix 4.2) tracked observed data for the various treatments across most years. Modeled soil respiration values reflected observations of higher rates from the labile manure compost early in the growing season, with modeled estimates within 1 g C/m²/d of most observations (Appendix 4.3). Modeled crop yields represented the lower values typically observed in the no fertilizer treatment, and most modeled values are within 100 g/m²/y of observed values (Appendix 4.4). The model captured interannual trends in soil organic matter across most treatments, including the decline in soil OM in the no fertilizer treatment and buildup in the high input municipal compost treatment (Appendix 4.5). Plant-available N (NO₃ + NH₄) showed seasonal spikes and declines that were represented in model output, although the magnitude of observed peaks often exceeded model predictions (Appendix 4.6). The model tracked observed values for plant-available P closely for some treatments (low input municipal compost, high input manure compost), while underpredicting values for high-input municipal compost and overpredicting values for no fertilizer, synthetic, and low-input manure treatments (Appendix 4.7). Modeled seasonal cumulative N leachate fluxes tracked observed values closely for 2017 and 2018, while underpredicting values for the following two years (Appendix 4.8). Modeled seasonal cumulative P leachate fluxes track observed values closely for some treatment-year combinations (e.g., 2017 synthetic, 2019 high-input manure, 2020 no-fertilizer, 2020 low-input manure, 2020 synthetic) while overpredicting some (e.g., 2018 and 2019 values for no fertilizer, synthetic, low-input municipal, and low-input manure treatments) and underpredicting others (2020 values for low-input municipal and high-input manure N). Modeled P leachate showed less among-treatment variation compared to observed values, but did reflect the relative differences among compost treatments, showing higher P leachate from the high-input labile manure compost compared to other organic amendments (Appendix 4.7).

In the independent verification dataset, the model correctly predicted lower crop harvest values in the no fertilizer treatment compared to other treatments. Model predictions for crop yields were somewhat lower compared to observed values for beans, collards, and peppers, but model predictions exceeded observed values for carrots. For years 1-4, cumulative harvest biomass ranged from 75 to 86% of observed values (Appendix 5.1). The model closely predicted leachate N fluxes for years 1 and 2, but under-represented N fluxes in years 3 and 4. Model predictions of cumulative N leachate fluxes from the first four growing seasons ranged from 2 to 67% lower compared to observed values (Appendix 5.2). Modeled leachate P fluxes tracked observed values in seasonal accumulation curves for five of the six experimental treatments. Modeled cumulative P leachate across the first for four growing seasons ranged from 54% lower to 57% greater than observed values for the four compost input treatments and the no fertilizer treatment. However, model predictions for P leachate loss from the synthetic fertilizer treatment was five-fold greater than observed values (Appendix

3.2. Results of sensitivity analysis

We examined the sensitivity of eight response variables across the different submodels to changes in parameter values (Appendix 6).

Cumulative ET was sensitive to field capacity, with a 50% decrease in field capacity resulting in a 92% decrease in ET. Cumulative ET was also sensitive to large changes in ks, which describes the relationship between soil moisture and ET. These same two parameters also control cumulative leachate: a 10% decrease in field capacity leads to a 40% increase in cumulative leachate, and a 10% decrease in ks results in an 11% increase in cumulative leachate. Cumulative harvest C shows sensitivity to 12 of the parameters tested across five of the different submodels, illustrating the interconnections among model currencies. This term showed highest sensitivity to field capacity, kLight, and kTempDecomp. Cumulative CO2 flux showed highest sensitivity to field capacity, all three of the decomposition rate submodel parameters (with highest sensitivity to kTempDecomp), as well as kRecalDecompFactor. Cumulative NUE and Cumulative N leachate responded to all of the parameters with the exception of the Phosphorus Submodel. These metrics showed largest responses to field capacity and ks (Hydrology Submodel), kLight (Plant Growth Submodel), and kTempDecomp (Decomposition Rate Submodel). Similarly, cumulative PUE was most sensitive to field capacity (Hydrology Submodel), kLight (Plant Growth Submodel), and kTempDecomp (Decomposition Rate Submodel). Cumulative P leachate was highly sensitive to field capacity and ks (Hydrology Submodel) and kPleachate (Phosphorus submodel), and showed small effects of nearly every other parameter, reflecting the many indirect connections throughout the model.

3.3. Results of 10-year input simulations

Plant-available N showed a characteristic seasonal buildup and drawdown (Fig. 1), peaking in late summer, approximately 100 days following annual compost application. The no-input scenario had the lowest levels of plant-available N, typically below 10 PPM. Low inputs of either municipal or manure compost generally reached 20 PPM, and higher compost inputs led to concentrations of plant-available N that were an order of magnitude higher (Fig. 2).

Plant-available P showed little to no seasonal signal, but medium and high inputs of compost resulted in steady long-term increases. For the no-input scenario, plant-available P concentration decreased from an initial value of 71 PPM to 48 PPM after ten years (Fig. 3). Low inputs of compost resulted in plant-available P stabilizing around 75 PPM (for

manure compost) to 90 PPM (municipal compost), while medium input levels resulted in sustained increases leading to concentrations around 160 PPM (manure compost) to 230 PPM (municipal compost) after a decade of inputs. High input rates led to steep increases in plant-available P, exceeding concentrations of 800 PPM (Fig. 3).

Over the 10-year simulation, N input ranged from 0 g N/m² in the noinput scenario, to 5500 g N/m² in the high-input scenarios (Table 1). For the no-input scenario, total N recovery was 121 g N/m², while leachate N loss totaled 19 g N/m². For the recalcitrant municipal compost, N recovery ranged from 157 g N/m² in the low-input scenario to 167 g N/m² in the high-input scenario, resulting in N use efficiency values of 40% (low input), 11% (medium input), and 3% (high input). Leachate N loss ranged from 19 g N/m² in the low-input scenario to 78 g N/m² in the high-input scenario. For labile manure compost, N recovery ranged from 164 g N/m² in the low-input scenario to 167 g N/m² in the high-input scenario, with N-use efficiencies ranging from 3 to 41%. Leachate N loss ranged from 48 g N/m² in the low-input scenario to 201 g N/m² in the high-input scenario (Table 1).

In the no-input scenario, over the 10 year simulation, $24 \,\mathrm{g \, P/m^2}$ were recovered as harvested crops, and $6 \,\mathrm{g \, P/m^2}$ were exported as leachate. With the addition of recalcitrant municipal compost, P inputs ranged from 56 to 764 g P/m², and P recovery ranged from 32 to 34 g P/m², resulting in P use efficiency values ranging from 4 to 57%. Leachate P loss ranged from 11 to 128 g P/m². With the addition of labile manure compost, P inputs ranged from 69 to 948 g P/m², and P recovery was 33–34 g P/m², resulting in P use efficiency values ranging from 4 to 48%. Leachate P loss values were approximately twice as high compared to the same input levels of recalcitrant municipal compost, ranging from 23 to 221 g P/m² (Table 1).

Carbon inputs ranged from 6200 to 85,800 g C/m² (recalcitrant municipal compost) and 12,200–167,800 g C/m² (labile manure compost) over ten years. Microbial respiration accounted for the fate of between one-third and two-thirds of organic carbon inputs, generating 3700–27,500 g C/m² (recalcitrant municipal compost) and 800–87,500 g C/m² (labile manure compost) as CO₂ emissions over ten years (Table 1). Carbon uptake by crop was significantly lower than CO₂ emissions from soil respiration, averaging 2400 g C/m² over 10 years.

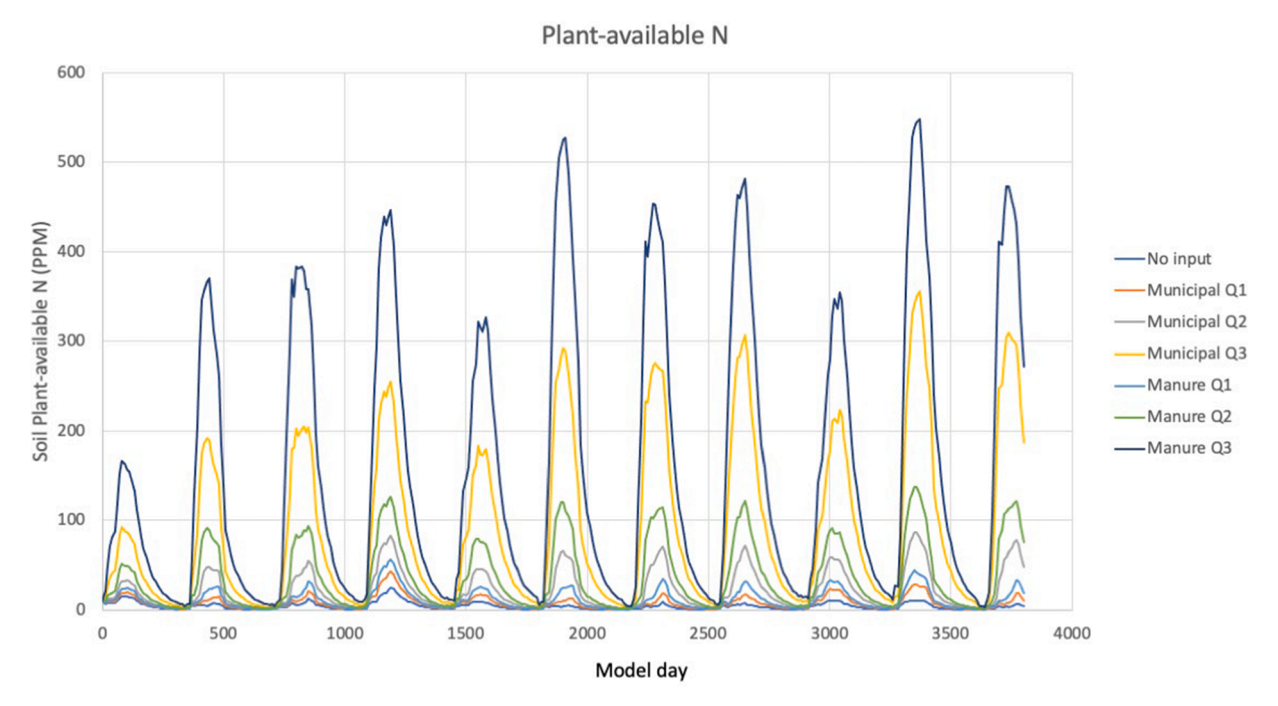


Fig. 2. Plant-available N (PPM) for the seven scenarios across the ten-year simulation period.

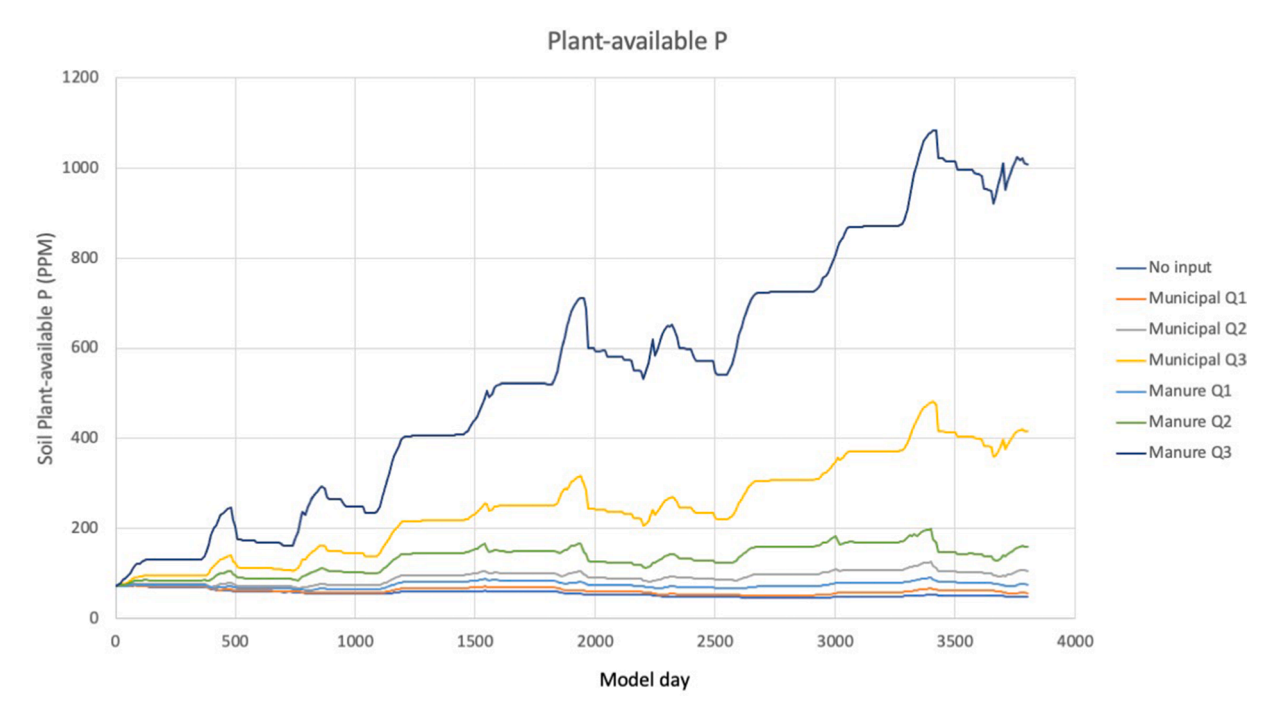


Fig. 3. Plant-available P (PPM) for the seven scenarios across the ten-year simulation period.

Table 1Compost characteristics and mass balance for nitrogen, phosphorus, and carbon over the 10-year simulation.

•		0 . 1 1						
Compost type Input level	none none	municipal low	municipal medium	municipal high	manure low	manure medium	manure high	
Compost C:N	_	15.6	15.6	15.6	30.5	30.5	30.5	
Compost N:P	_	7.2	7.2	7.2	5.8	5.8	5.8	
Compost% labile	-	25	25	25	50	50	50	
N input $(g/m^2/10y)$	0	400	1400	5500	400	1400	5500	
Harvest N (g/m ² /10y)	121	158	166	167	164	167	167	
N leachate (g/m ² /10y)	19	33	78	154	48	120	201	
N-use efficiency (%)		40	11	3	41	12	3	
P input (g/m ² /10y)	0	56	194	764	69	241	948	
Harvest P (g/m²/10y)	24	32	34	34	33	34	34	
P leachate (g/m ² /10y)	6	11	38	128	23	92	221	
P-use efficiency (%)		57	17	4	48	14	4	
C input $(g/m^2/10y)$	0	6200	21,800	85,800	12,200	42,700	167,800	
CO_2 flux (g/m ² /10y)	2000	3700	8200	27,500	8000	23,200	87,500	
Harvest C (g/m²/10y)	1800	2300	2400	2500	2400	2500	2500	

3.4. Results of N and P tracer simulation

Of the N in soil organic matter at the start of the experiment, a maximum of 33% was recovered in harvested biomass in the no-input treatment, with minimum values of $5{\text -}6\%$ in the high compost input treatments (Fig. 4). Most of this recovery occurred during the first three growing seasons. Cumulative leachate losses ranged from 3% (municipal compost–low input) to 9% (manure compost–medium input), with nearly all of losses occurring during the first three years (Fig. 5). The no-input treatment lost a larger fraction of initial soil organic N (5%) than did any of the municipal compost treatments.

Crops recovered between 8% (high input manure compost) to 33% (no-input) of the initial P in soil organic matter, with this cumulative amount increasing steadily over the ten-year simulation (Fig. 6). For low, medium, and high input rates of municipal compost, <1% of the initial organic P was exported as leachate, compared to 8% in the no-input treatment. Manure compost yielded larger relative export as leachate, with 39% of this pool lost as leachate over a decade in the high-input manure compost treatment. Losses continued at a fairly steady rate over the simulated ten-year period (Fig. 7).

4. Discussion

4.1. Evaluation of model performance

While numerous other models of soil organic matter and biogeochemistry have been developed for grassland and conventional agricultural systems (e.g., Campbell and Paustian 2015, Berardi et al., 2020), our model focuses on the dynamics of small scale urban vegetable gardens with specific focus on compost inputs, using 5+ years of empirical data. We note that similar datasets are now being collected in other urban gardens in different parts of the world (e.g., Sieczko et al., 2022), which will allow for further verification and improvement of this model, and in turn, the model can facilitate cross-site comparisons. The one-day time step in this model differs from the monthly time step in many other soil models (Campbell and Paustian 2015), providing temporal resolution needed to simulate individual rain events. The model is of moderate complexity, potentially allowing for use by a variety of stakeholders across different outdoor urban agriculture systems.

The model was generally able to represent the coupled dynamics of water, carbon, nitrogen, and phosphorus, in urban garden

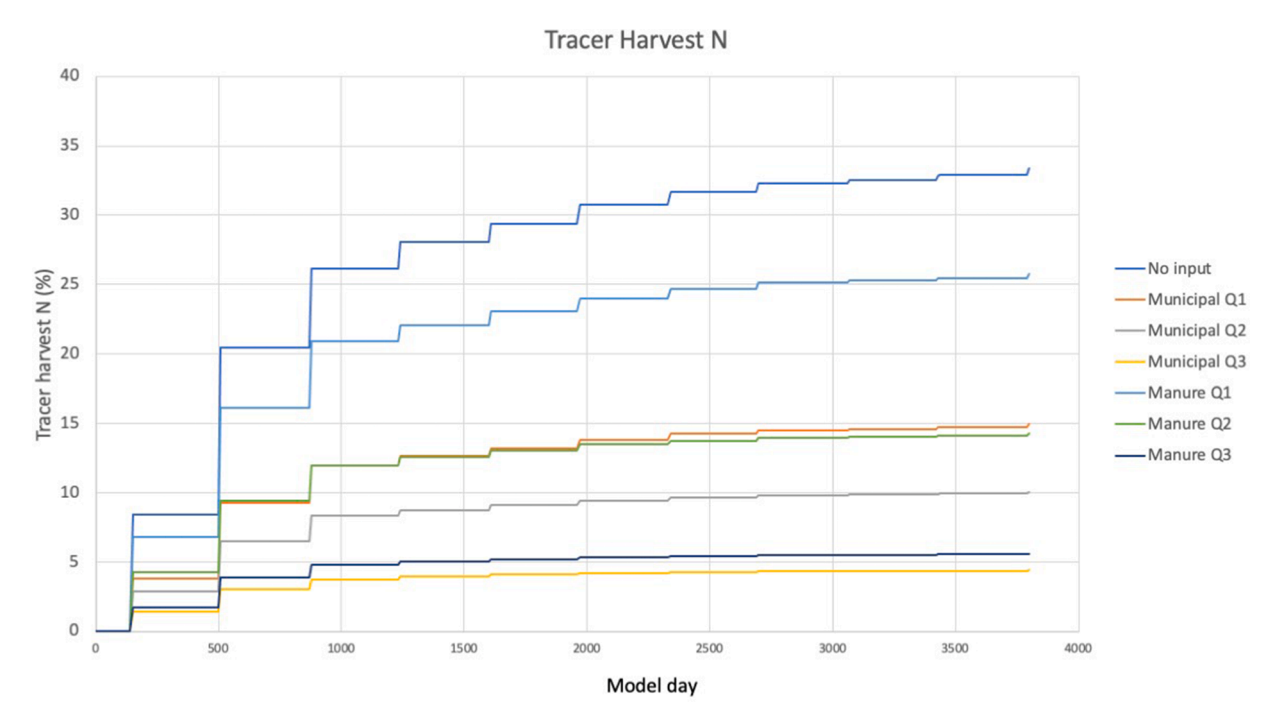


Fig. 4. Percent of N in soil organic matter at beginning of experiment that is ultimately removed as harvested biomass.

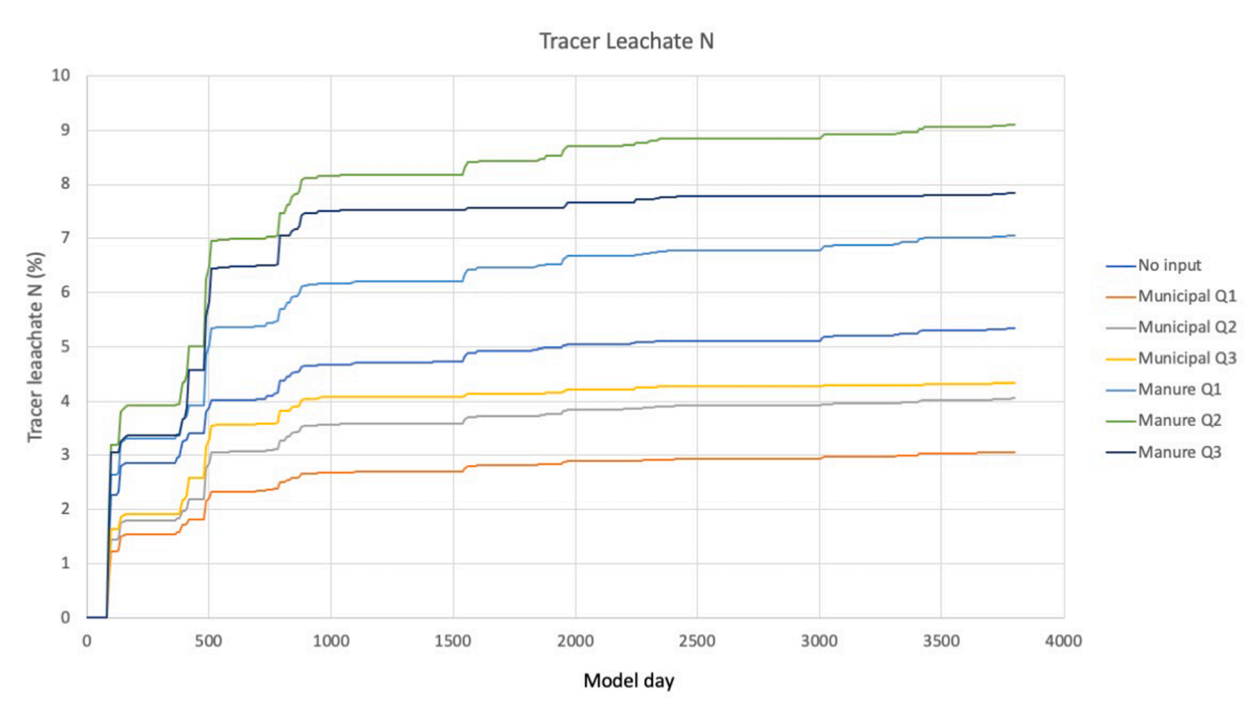


Fig. 5. Percent of N in soil organic matter at beginning of experiment that is ultimately exported as leachate.

agroecosystems. Although we have an extensive amount of empirical data from six years of measurements (Small & Shrestha 2023), this ecosystem model synthesizes these data and allows for additional insights into system behavior, by examining additional input scenarios, examining longer-term trajectories, and following the fate of initial inputs to the system.

While it overrepresented the accumulation and leachate flux of P from the synthetic fertilizer treatment, the model was closer to observed values for the four compost amendment treatments. Moreover, there are several reasons why observed values are imperfect comparisons. Stochastic factors such as insect herbivory affected observed crop yields in

ways that were not represented in the model. The model assumes homogeneity of fluxes over the $1\mathrm{m}^2$ area, and of stocks between soil depths of 0–30 cm, but spatial heterogeneity certainly influences observed readings. The 128 lysimeters collected leachate from just over 1% of garden area, so any pooling of water or other non-uniform flows would bias the observed leachate data. Extrapolation is also a potential source of error for soil respiration, as here we are using fluxes measured from short-term (3 min) observations to estimate daily rates needed for the model's 1 day dt. Biweekly samples collected for soil nutrients and organic matter represented the top 10 cm of the soil column, and soil moisture is also measured at 10 cm, whereas the model represents the

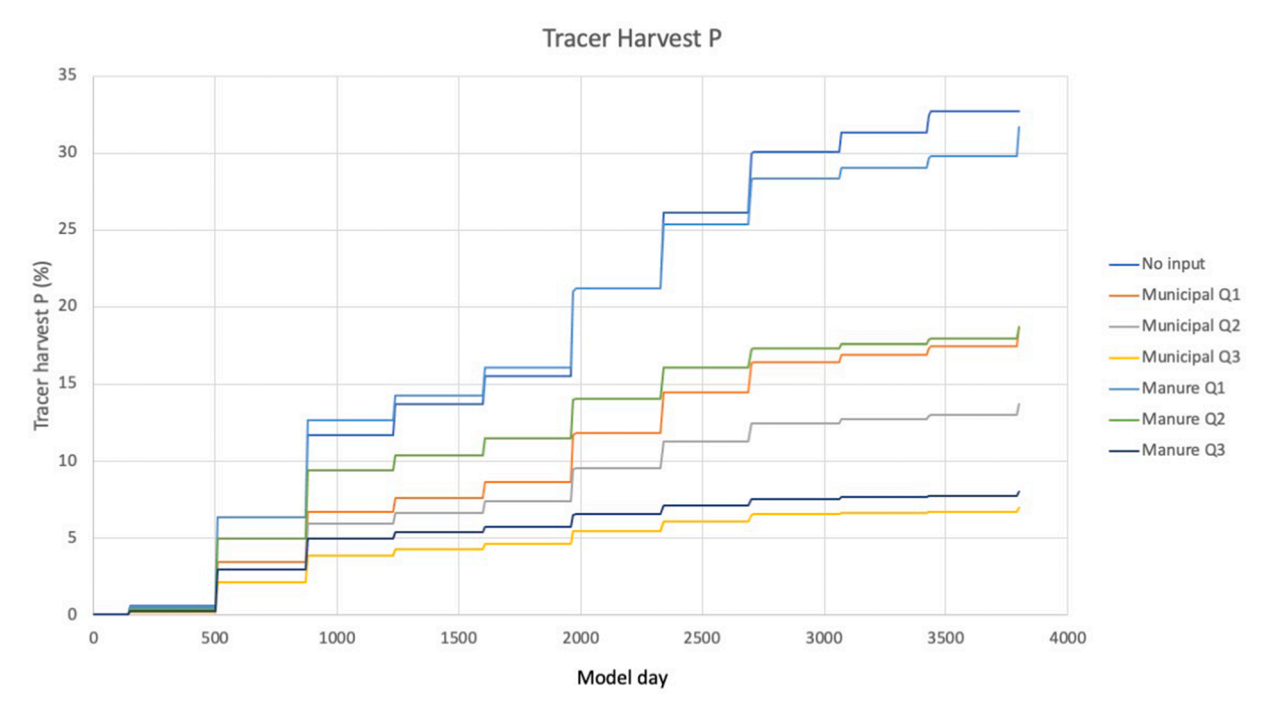


Fig. 6. Percent of P in soil organic matter at beginning of experiment that is ultimately removed as harvested biomass.

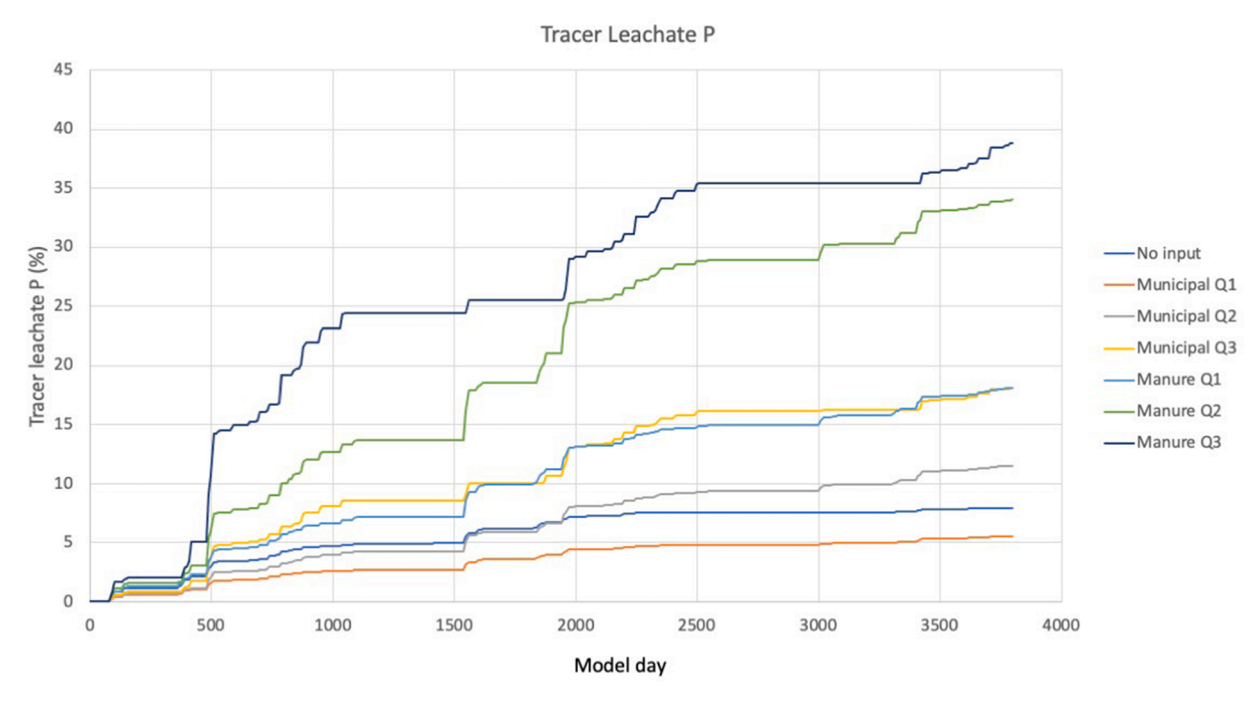


Fig. 7. Percent of P in soil organic matter at beginning of experiment that is ultimately exported as leachate.

top 30 cm, so any differences in chemistry of deeper soil layers would be perceived as error. Empirical data are lacking for some other potentially important fluxes (e.g., dissolved organic C, N, and P in leachate; gaseous N losses). Nevertheless, the model typically captured temporal trends and differences among treatments, representing observed values within a factor of two in most cases.

4.2. Coupled dynamics of model currencies

While the research questions underlying this study focus on the fate of P, the dynamics of this element are dependent upon the fate of the

other model currencies. The previously published hydrology submodel (Chapman et al., 2022) illustrates how soil organic matter levels affect the capacity for water retention in the soil, and ultimately controls the fraction of water exported via evapotranspiration vs. leachate. Here, we show more fully the interconnections among these sub-models, as illustrated by the sensitivity analysis showing how the fate of P is affected by parameter values across all submodels, and particularly strongly controlled by hydrologic parameters (Appendix 6.2). Soil moisture is an important control on both organic matter decomposition and crop growth, affecting the supply and demand, respectively, of plant-available N and P. Compost inputs and plant root exudates

contribute organic matter to soils, while microbial decomposition consumes organic carbon and makes N and P available for plants. Because N is the limiting nutrient for crop growth, N-availability in turn affects plant biomass and plant uptake of P. Plants are effectively "competing" with leachate for the pool of plant-available N and P, and the magnitude of plant uptake and leachate can be similar in high-input scenarios, as our empirical data have previously shown (Small et al., 2018). The timing and frequency of intense rain events is therefore an important control on nutrient export via leachate, and it is notable that climate scenarios predict increases in rainfall during spring and fall (Easterling et al., 2017) and an increase in magnitude of extreme precipitation events (Hayhoe et al., 2010).

4.3. Effects of management decisions on nutrient recycling and loss

Management decisions made by gardeners—especially input rates of nutrients as compost or inorganic fertilizer—are the most important driver of nutrient dynamics. Many urban gardeners apply high levels of compost year after year, adding P at levels far higher than crops can use (Small et al., 2019a). Because P is relatively immobile, much of this excess is stored in the soil, but eventually the capacity of garden soil to hold additional P becomes diminished, as has been seen in a 150-year empirical study of manure amendments to farm plots in the United Kingdom (Heckrath et al., 1995). Not only does the mass of N and P applied affect storage and export, but the lability of these inputs is also an important control on the fate of these nutrients. The addition of nutrients in recalcitrant municipal compost results in a slower release of nutrients to the plant-available pool, resulting in lower losses to leachate and a higher fraction of nutrients ultimately recovered by crops.

The slow release of organic P in this garden ecosystem coupled with the capacity of soil to retain this excess P results in a long potential time lag that decouples relationships between inputs and outputs. Model results show that, at realistic compost input levels (50th and 75th percentile application rates from Small et al., 2019a), plant-available P accumulates in the soil faster than it can be taken up by crops. This model output corresponds with the empirical relationship between garden age and soil P documented in Small et al. (2019a). Previous empirical studies have found that there is little or no relationship between compost P inputs and soil P leachate at short timescales (van de Vlasakker et al. 2022) and that the dominant short-term fate of excess compost-derived P is soil storage rather than leachate export (Shrestha et al., 2020). The model output from the simulated tracer study provides insight into the longer-term fate of this P. Compost-derived P still contributes to crop uptake and leachate a decade after the compost was originally added to the garden (Fig. 6, Fig. 7), and generates nearly as much leachate between years 6-10 as it does in the first five years. By contrast, compost-derived N is mostly taken up by crops or exported via leachate within three years of compost addition (Fig. 4, Fig. 5). Ultimately, this "legacy P" (sensu Sharpley et al., 2013) exceeds capacity for soil retention, and P lost through runoff may be an important contributor to eutrophication in freshwater ecosystems. A previous spatial model (Small et al., 2023) showed that compost applied to vegetable gardens across an urban landscape may account for a large fraction of total urban P runoff, but the results of this model, which assumes steady-state dynamics, were highly sensitive to soil P retention, which is a dynamic property. The results of the current model simulations provide new insight into the temporal dynamics that ultimately determines what fraction of P applied as compost is recycled into crops, stored indefinitely, or exported as leachate or runoff.

While the application of compost to gardens is considered to be generally considered to be a beneficial reuse of nutrients bound in organic waste, the model results illustrate that a small fraction of compost-derived N and P are ultimately recovered by crops. Between 5–25% of N is recovered by crops within a decade (Fig. 3), and 8–30% of P is ultimately recycled (Fig. 5). Higher compost inputs invariably result in lower recovery efficiency, and at high compost inputs, a larger mass of

N and P are ultimately lost as leachate (Fig. 5, Fig. 7) than are recovered by crops (Fig. 4, Fig. 6). These results underscore tradeoffs among potential ecosystem services that may be desired for urban gardens such as serving as a sink for recycled nutrients, maximizing crop yield, and improving water quality through infiltration. Such tradeoffs are not inevitable, however: our previous empirical results (Shrestha et al., 2020), as well as the results of this model, show that targeting compost application rates to crop nutrient demand maintains high crop yields while resulting in relatively high nutrient use efficiency and low nutrient leachate export. Our intention is that this model can help inform stakeholder decisions in optimizing desired ecosystem services from urban agriculture.

Irrigation is another garden management decision that can have important implications for the fate of P within the garden agroecosystem. Because some urban gardeners have limited or no access to municipal water (Wortman and Taylor Lovell 2013), it is likely that there is a wide range of irrigation practices. We previously showed that evapotranspiration is the dominant fate of water inputs from irrigation (Chapman et al., 2022), but even if evapotranspiration is not contributing directly to leachate, keeping soil moisture at higher levels likely reduces capacity for water retention from a significant rain event, ultimately leading to higher leachate fluxes of water and associated nutrients. Higher soil moisture levels also increase rates of organic matter decomposition and crop growth, ultimately increasing rates of many of the flows in the garden agroecosystem.

Our model also allows us to explore the potential contribution of urban gardens as C sinks, potentially offsetting some of the high C emissions from combustion of fossil-fuel in cities. The model results illustrate some of the nuance in C offset calculations, as results depend on which fluxes are considered. While high compost inputs does lead to accumulation of organic C, about half of this total is ultimately respired, contributing CO2 back to the atmosphere. Crop growth is a sink for C, but plant CO2 uptake removes only around one-tenth of the mass of C respired by soil microbes, and much of the C in harvested crops will ultimate be consumed and respired by humans. Over ten years, a garden receiving high compost inputs could accumulate (after accounting for respiration losses) approximately 40 kg C/m² (147 kg CO₂/m²). By comparison, the net C sequestration of a single urban tree is 300-2500 kg CO₂/10y (Pataki et al., 2006), so on an areal basis, high-input gardens may have 5-50% of the C sequestration potential of an urban tree. However, C mitigation by urban greenspace remains much smaller in magnitude compared to anthropogenic emissions (Strohbach et al.,

5. Conclusions

Whether composting coupled with urban agriculture can be scaled to recycle a significant amount of nutrients from organic waste back into the human food system depends on the stoichiometric balance between limiting and non-limiting nutrients, and the dynamic conditions in garden soil that control whether these nutrients are stored, taken up by crops, or lost to the environment. This model is an attempt to better understand these dynamics, through simulating the coupled biogeochemical cycling of C, N, P, and water in an urban agroecosystem. While experimental data have indicated that high input compost addition to urban gardens results in a long-term build-up and export of P, the temporal dynamics of this process has been obscured in empirical snapshots. The amount of P leaching from garden soils into urban water flow paths ultimately depends on the capacity of soil to retain excess P, which is a dynamic process. This model provides insight into the physical, chemical, and biological factors that control this process, and provides a tool to predict how compost input rates may control the fraction of nutrients recycled vs. exported at decadal timescales. These findings underscore the need for consideration of mass balance constraints in expanding urban organics waste recycling programs.

CRediT authorship contribution statement

Gaston E. Small: Conceptualization, Methodology, Validation, Investigation, Writing – original draft, Project administration, Funding acquisition. Marisa Smedsrud: Software, Formal analysis, Data curation, Writing – review & editing. Ivan Jimenez: Software, Investigation. Eric Chapman: Investigation, Supervision, Writing – review & editing.

Declaration of Competing Interest

The authors declare that they have no known competing financial vinterests or personal relationships that could have appeared to influence the work reported in this paper.

Data availability

Data and code are included in appendix. Original data are published in EDI

Acknowledgments

This work was supported by a National Science Foundation CAREER award (award number 1651361) to GES, and by the Minneapolis-St. Paul Metropolitan Area (MSP) Long-Term Ecological Research Program (NSF award number 2045382). MS and IJ were supported by a summer research grant from the University of St. Thomas Center for Applied Mathematics.

Supplementary materials

Supplementary material associated with this article can be found, in the online version, at doi:10.1016/j.ecolmodel.2023.110441.

References

- Aoyama, M., Nozawa, T., 2012. Microbial biomass nitrogen and mineralizationimmobilization processes of nitrogen in soils incubated with various organic materials. Soil Sci. Plant. Nutr. 39, 23–32.
- Berardi, D., Brzostek, E., Blanc-Betes, E., Davison, B., DeLucia, E.H., Hartman, M.D., Kent, J., Parton, W.J., Saha, D., Hudiburg, T.W., 2020. 21st-century biogeochemical modeling: challenges for Century-based models and where do we go from here? GCB Bioenergy 12 (10), 774–788.
- Burger, J.R., Allen, C.D., Brown, J.H., Burnside, W.R., Davidson, A.D., Fristoe, T.S., Hamilton, M.J., Mercado-Silva, N., Nekola, J.C., Okie, J.G., Zuo, W., 2012. The macroecology of sustainability. PLOS Biol. 10, e1001345.
- Cambardella, C.A., Richard, T.L., Russell, A., 2003. Compost mineralization in soil as a function of composting process conditions. Eur. J. Soil Biol. 39, 117–127.
- Campbell, E.E., Paustian, K., 2015. Current developments in soil organic matter modeling and the expansion of model applications: a review. Environ. Res. Lett. 10, 123004
- Chang, E.H., Chung, R.S., Tasi, Y.H., 2010. Effect of different application rates of organic fertilizer on soil enzyme activity and microbial population. Soil Sci. Plant. Nutr. 53, 132–140.
- Chapman, E.J., Small, G.E., Shrestha, P., 2022. Investigating potential hydrological ecosystem services in urban gardens through soil amendment experiments and hydrologic models. Urban Ecosyst. 25, 867–878.
- Childers, D.L., Corman, J., Edwards, M., Elser, J.J., 2011. Sustainability challenges of phosphorus and food: solutions from closing the human phosphorus cycle. Bioscience 61, 117–124.
- Chtouki, M., Laaziz, F., Naciri, R., Garré, S., Nguyen, F., Oukarroum, A., 2022. Interactive effect of soil moisture content and phosphorus fertilizer form on chickpea growth, photosynthesis, and nutrient uptake. Sci. Rep. 12, 6671. UK.
- Chu, H., Lin, X., Fujii, T., Morimoto, S., Yagi, K., Hu, J., Zhang, J., 2007. Soil microbial biomass, dehydrogenase activity, bacterial community structure in response to longterm fertilizer management. Soil Biol. Biochem. 39, 2971–2976.
- Cofie, O.O., Veenhuizen, R.V., Dreschel, P., 2003. Contribution of urban and peri-urban agriculture to food security in sub-Saharan Africa. In: Proceedings of the Africa Session of 3rd WWF, 17 March 2003. Kyoto.
- Di, H.J., Cameron, K.C., 2002. Nitrate leaching in temperate agroecosystems: sources, factors and mitigating strategies. Nutr. Cvcl. Agroecosystems 64, 237–256.
- factors and mitigating strategies. Nutr. Cycl. Agroecosystems 64, 237–256. Easterling, D.R., Arnold, J.R., Knutson, T., Kunkel, K.E., LeGrande, A.N., Leung, L.R., Vose, R.S., Waliser, D.E., Wehner, M.F., 2017. Precipitation change in the United States. Fourth National Climate Assessment 1.

- Graefe, S., Schlecht, E., Buerkert, A., 2008. Opportunities and challenges of urban and peri-urban agriculture in Niamey, Niger. Outlook Agr. 37, 47–56.
- Hayhoe, K., Sheridan, S., Kalkstein, L., Greene, S., 2010. Climate change, heat waves, and mortality projections for Chicago. J. Gt. Lakes Res. 36, 65–73. https://doi.org/ 10.1016/j.jglr.2009.12.009.
- Heckrath, G., Brookes, P.C., Poulton, P.R., Goulding, K.W.T., 1995. Phosphorus leaching from soils containing different phosphorus concentrations in the Broadbalk Experiment. J. of Environ. Qual. 24, 904–910.
- Jørgensen, S.E., Bendoricchio, G., 2001. Fundamentals of Ecological Modelling In: Developments in Environmental Modelling, 3rd Ed., 21. Elsevier, Amsterdam.
- Kleinman, P.J.A., Allen, A.L., Needelman, B.A., Sharpley, A.N., Vadas, P.A., Saporito, L. S., Folmar, G.J., Bryant, R.B., 2007. Dynamics of phosphorus transfers from heavily manured coastal plain soils to drainage ditches. J. Soil Water Conserv. 62, 225–235.
- Kleinman, P.J.A., Sharpley, A.N., McDowell, R.W., Flaten, D.N., Buda, A.R., Tao, L., Bergstrom, L., Zhu, Q., 2011. Managing agricultural phosphorus for water quality protection: principles for progress. Plant Soil 349, 169–182.
- Luu, A.T., Hoang, N.T., Dinh, V.M., Bui, M.H., Grandy, S., Hoang, D.T., 2022. Effects of carbon input quality and timing on soil microbe mediated processes. Geoderma 409, 115605.
- Metson, G.S., Bennett, E.M., 2015. Phosphorus cycling in montreal's food and urban agriculture systems. PLOS One 10, e0120726.
- Minasny, B., McBratney, A.B., 2017. Limited effect of organic matter on soil available water capacity. Eur. J. Soil Sci. 69, 39–47.
- Minnesota DNR, 2003. Past climate data for minnesota. https://www.dnr.state.mn. us/climate/historical/daily-data.html?sid=mspthr&sname=Minneapolis/St% 20Paul%20Threaded%20Record&sdate=2010-01-01&edate=por. (Accessed 2023-04-20).
- Pataki, D.E., Alig, R.J., Fung, A.S., Golubiewski, N.E., Kennedy, C.A., McPherson, E.G., Nowak, D.J., Pouyat, R.V., Romero Lankao, P., 2006. Urban ecosystems and the North American carbon cycle. Glob. Change Biol. 12, 2092–2102.
- Rees, W.E., Wackernagel, M., Jansson, A., Hammer, M., Folke, C., Costanza, R., 1994.
 Appropriated carrying capacity: measuring the natural capital requirements of the human economy. Investing in Natural Capital: Ecological Economics Approach to Sustainability. Island Press, Washington, D.C.
- Saher, R., Shephen, H., Ahmad, S., 2021. Urban evapotranspiration of green spaces in arid regions through two established approaches: a review of key drivers, advancements, limitations, and potential opportunities. Urban Water J. 18, 115–127.
- Sandhu, S., Sekaran, U., Ozlu, E., Hoilett, N.O., Kumar, S., 2019. Short-term impacts of biochar and manure application on soil labile carbon fractions, enzyme activity, and microbial community structure. Biochar 1, 271–282.
- Sieczko, A.K., van de Vlasaker, P., Tonderski, K., Metson, G.S., 2022. Seasonal nitrogen and phosphorus leaching in urban agriculture: dominance of non-growing season losses in a Southern Swedish case study. Urban For. Urban Green. 79, 127823.
- Sharpley, A., Jarvie, H.P., Buda, A., May, L., Spears, B., Kleinman, P., 2013. Phosphorus legacy: overcoming the effects of past management practives to mitigate future water quality impairment. J. Environ. Oual. 42, 1308–1326.
- Shrestha, P., Small, G.E., Kay, A., 2020. Quantifying nutrient recovery efficiency and loss from compost-based urban agriculture. PLOS One 15 (4), e0230996.
- Small, G.E., Shrestha, P., Kay, A., 2018. The fate of compost-derived phosphorus in urban gardens. Int. J. Des. Nat. Ecodynamics 13 (4), 415–422. https://doi.org/10.2495/ DNF-V13-N4-415-422.
- Small, G.E., Shrestha, P., Metson, G.S., Polsky, K., Jimenez, I., Kay, A., 2019a. Excess phosphorus from compost applications in urban gardens creates potential pollution hotspots. Environ. Res. Comm. 1, 091007 https://doi.org/10.1088/2515-7620/ ab3b8c.
- Small, G.E., Osborne, S., Shrestha, P., Kay, A., 2019b. Measuring the fate of compostderived phosphorus in native soil below urban gardens. Int. J. Environ. Res. Pub. He. 16, 3998. https://doi.org/10.3390/ijerph16203998.
- Small, G., Jimenez, I., Salzl, M., Shrestha, P., 2020. Urban heat island mitigation due to enhanced evapotranspiration in an urban garden in Saint Paul, Minnesota, USA. WIT Trans. Ecol. Environ. 243, 39–45.
- Small, G.E., Shrestha, P., 2023. Influence of soil amendment and crop species on nutrient cycling in a St. Paul urban garden ver 2. Environ. Data Initiat. https://portal.edire pository.org/nis/mapbrowse?scope=edi&identifier=1098&revision=2, 2006 Accessed 2023-04-20.
- Small, G.E., Martensson, N., Janke, B.D., Metson, G.S., 2023. Potential for high contributions of urban gardens to nutrient export in urban watersheds. Landsc. Urban Plan. 229, 104602.
- Smith, O.B., 2001. Overview of Urban Agriculture and Food Security in West Africa. International Development Research Centre, Ottawa, Canada.
- Strohbach, M.W., Arnold, E., Haase, D., 2012. The carbon footprint of urban green space–A life cycle approach. Landsc. Urban Plan. 104, 220–229.
- Turner, B.L., Haygarth, P.M., 2000. Phosphorus forms and concentrations in leachate under four grassland soil types. Soil Sci. Soc. Am. J. 64, 1090–1099.
- van de Vlasakker, P.C.H., Tonderski, K., Metson, G.S., 2022. A review of nutrient losses to waters from soil- and ground-based urban agriculture—More nutrient balances than measurements. Front. Sustain. Food Syst. https://doi.org/10.3389/ fsufs.2022.842930.
- Wielemaker, R., Oenema, O., Zeeman, G., Weijma, J., 2019. Fertile cities: nutrient management practices in urban agriculture. Sci. Total Environ. 668, 1277–1288.
- Wortman, S., Taylor Lovell, S., 2013. Environmental challenges threatening the growth of urban agriculture in the United States. J. Environ. Qual. 42, 1283–1294.

- Xing, G.X., Zhu, Z.L., 2000. An assessment of N loss from agricultural fields to the environment in China. Nutr. Cycl. Agroecosystems 57, 67–73.
 Yuste, J.C., Baldocchi, D.D., Gershenson, A., Goldstein, A., Misson, L., Wong, S., 2007.
 Microbial soil respiration and its dependency on carbon inputs, soil temperature and moisture. Global Change Biol. 13, 2018–2035.
- Zotarelli, L., Dukes, M.D., Romero, C.C., Migliaccio, K.W., 2010. Step By Step Calculation of the Penman-Monteith Evapotranspiration (FAO-56 Method). Institute of Food and Agricultural Sciences. University of Florida, p. 8.